



EXPERIMENTAL AND NUMERICAL STUDY OF THE DYNAMICAL BEHAVIOR OF E-GLASS/VINYLESTER COMPOSITES SUBJECTED TO IN-PLANE AND OUT-OF-PLANE HIGH STRAIN RATE COMPRESSIVE LOADING

J. ARBAOUI^{1*}, M. TARFAOUI¹ and A. EL MALKI¹

¹ENSTA-Bretagne, MSN/LBMS/DFMS, 2 rue François Verny 29806 Brest, France

Email: jamal.arbaoui@ensta-bretagne.fr, mostapha.tarfaoui@ensta-bretagne.fr,
aboulghit.el_malki_alaoui@ensta-bretagne.fr

ABSTRACT

Split Hopkinson Pressure Bar (SHPB) is one of the most important and recognized apparatus used for characterizing the dynamic behavior of materials. In the first part, the results from a series of SHPB tests on the woven composites are presented in this paper. These tests were done in two configurations: in-plane and out-of-plan compression test. It is observed that the failure strength varies with the different loading directions. The results indicate that the stress-strain curves, maximum compressive stresses and strains evolve as strain rate changes. In the second part of this study, numerical models without damage are developed to investigate the validity of assumptions of compression Split-Hopkinson Pressure Bar technique. Abaqus software was used for the numerical simulation. The results obtained by numerical investigation (finite elements) of SHPB are compared with the in-plane and out-of-plan compression test of a woven composite. A good correlation was noted between the experimental and numerical results which allows validate the numerical approach used.

1 INTRODUCTION

Composite materials exhibit favorable mechanical properties over metallic materials and hence are increasingly considered for high technology applications, particularly in the naval field. Some of these applications are in structures subjected to dynamic loads. Since behavior of composites is known to depend on the rate of loading, knowledge of the constitutive behavior and dynamic strength (which is usually higher than the static value) is highly desirable for designers of structures intended to withstand dynamic loads [1]. Dynamic behavior of materials in the range of $100\text{--}10000\text{ s}^{-1}$ strain rates has been widely studied by the Split Hopkinson's Pressure Bars (SHPB) [2]. Griffiths and Martin [3] investigated the dynamic behavior of unidirectional carbon fiber composites at high strain rates to determine how the material behavior is dependent on fiber volume fraction and fiber orientation. Chen et al. [4] investigated the effect of strain rate on the compressive and tensile behavior of a 0/90 carbon fiber reinforced resin matrix composite. Hosur et al. [5] tested the compressive properties of carbon/epoxy laminated composites at three different strain rates of 82, 164 and 817 s^{-1} along in-plane directions. Elanchezhian et al. [6] studied the effect of varying strain rates and temperatures on the Mechanical behavior of glass and carbon fiber reinforced composites. Sierakowski et al. [7] investigated steel/epoxy composites in compression up to 1000 s^{-1} . Jenq and Sheu [8] examined the high strain rate behavior of stitched and unstitched glass/epoxy composites. Tarfaoui et al. [9, 10] tested the mechanical behaviors of angle-ply (0° , $\pm 20^\circ$, $\pm 30^\circ$, $\pm 45^\circ$, $\pm 60^\circ$, $\pm 70^\circ$ and 90°) plain weave composite laminates subjected to in-plane and out-of-plane high strain rate compressive loading. The stress-strain curves of the composite laminates showed that the material is strongly sensitive to fiber orientation and loading direction. El-Habak [11] studied the mechanical behavior of woven glass fiber reinforced composites at failure strain rates ranging from 100 to 1000 s^{-1} . He studied the effect of sizing of the fiber, and two different resin systems: epoxy and vinylester. He found that, while sizing did not influence the high strain rate behavior, composites made of vinylester matrix yielded higher strength. Woldenbet and Vinson [12] studied the effect of specimen geometry in high strain rate testing of graphite/epoxy laminates. Harding [13] studied two woven glass/ epoxy material systems in compression up to 860 s^{-1} using cylindrical and thin strip specimens. The results for both specimen geometries indicated a significant increase in the initial modulus, strength and strain to failure with increasing strain rate.

In the present work, in-plane and out-of-plane compression behavior of an E-glass fiber reinforced vinylester composite at high strain rates was determined. Composite were prepared in $0^\circ/90^\circ$ orientation by using infusion process, tested in Split Hopkinson Pressure Bar apparatus, and modeled with explicit commercial finite element code Abaqus [14].

2 EXPERIMENTAL PROCEDURE

The woven E-glass/vinylester laminate composites samples used in our experiment were provided by EADS Composites and were manufactured for the naval applications. The sample has 52 layers with a vinylester resin matrix DION 9102. Each layer is a plain weave construction (50% weft yarns per 50% warp yarns) made of E-glass fabric, which create orthotropic mechanical properties in the three orthogonal directions. The thickness of the samples is 10.0 mm and their density is 1.85 g/cm^3 . The overall fiber volume fraction is 49% for the composite. The physical and mechanical properties of the vinylester resin and E-glass fibers are shown in Table 1. For dynamic tests, the cubic specimens with side length 10.0 mm for out-of-plane and 13.0 mm for in-plane loading tests, are considered, respectively. The specimen and loading direction, in-plane, and out-of-plane are presented in Figure 1. The faces

of the specimens were polished with 1000-grit sandpaper to ensure parallel loading edges. To avoid uncertainties related to size effects, the specimens in all the tests are of the same geometry.

| Characteristic | E-glass fiber | Vinylester resin |
|--------------------------------|---------------|------------------|
| Density (kg/m^3) | 2540 | 1050 |
| Young modulus in tension (MPa) | 74000 | 80 |
| Shear modulus (GPa) | 33.3 | 1.24 |
| Poisson Coefficient | 0.22 | 0.35 |
| Tensile strength (MPa) | 2400 | 80 |
| Compressive strength (MPa) | 1450 | 115 |

Table 1. Characteristics of the E-glass fiber and the vinyl ester resin

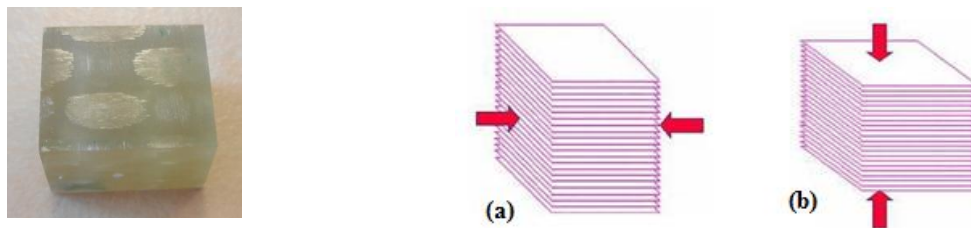


Figure 1. Specimen and loading direction, (a) in-plane and (b) out-of-plane

3 EXPERIMENTAL RESULTS

In these dynamic compression tests, a cubic sample of size $13 \text{ mm} \times 13 \text{ mm} \times 10 \text{ mm}$, is placed between the two bars, of the same diameter of 20 mm. The striker, incident and transmitted bars have a length of 400 mm, 1985 mm and 1845 mm, respectively. These bars are correctly aligned and are able to slide freely in the frame of the apparatus. The composite specimen is not attached to the bar in order to prevent the perturbation of measurement due to additional interfaces, Figure 2.

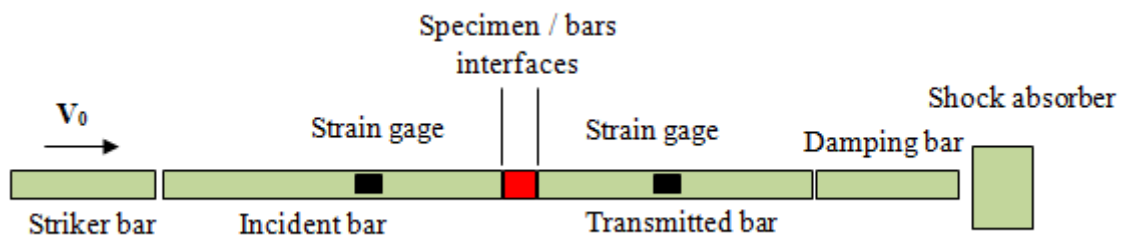


Figure 2. Schematic of compression SHPB set-up.

Before conducting the dynamic tests on the Hopkinson bar, it is necessary to ensure that these tests can be reproduced. With this objective in mind, for each loading direction, a minimum of two tests were carried out at the same impact pressure in order to analyze the tests reproducibility. As Figure 3 shows, it is noted that the tests are repeatable and this was checked for each test. For in-plane and out-of-plane tests, results for compressive strain rate between 293 s^{-1} and 1902 s^{-1} are obtained using SHPB.

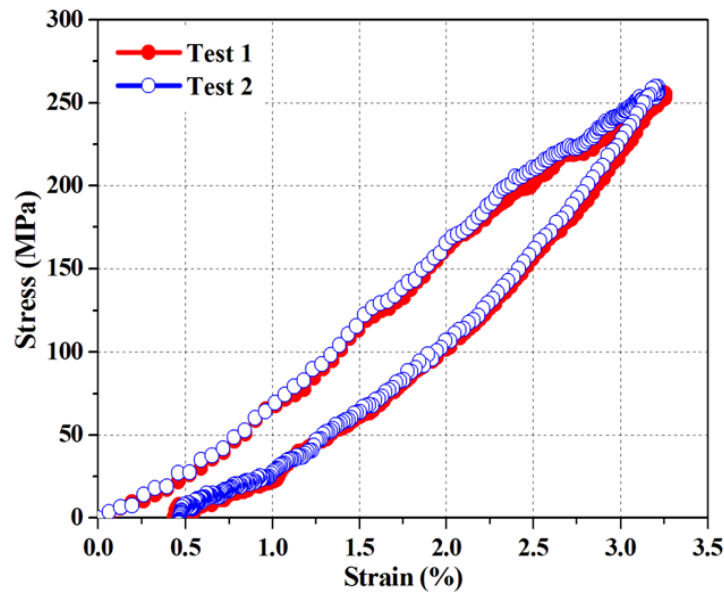


Figure 3. Test reproducibility, $P=0.1$ MPa – $V=8.29$ m/s

3.1 In-plane test

3.1.1 Mechanical behavior

The laminate specimens $[0/90]_{26}$ were subjected to in-plane loading with nine different impact pressures of the striker bar on the incident bar: 0.5, 0.7, 1, 1.2, 1.5, 1.7, 2, 2.2 and 2.5 bar (50, 70, 100, 120, 150, 170, 200, 220 and 250 ($\times 10^{-3}$ MPa)). The typical strain rate-time obtained from tests on the Hopkinson bar is shown in Figure 4. The strain rate evolution is sensitive to the entry pressure P in the chamber of compressed air and the loading direction. In the first phase, the strain rate increases rapidly, then decreases and remains fairly constant for an impact pressure from 0.5 to 1.7 bar. Indeed, the increase in impact pressure shows that the strain rate is not constant in the second phase. The presence of a second peak is the principal characteristic of these curves, which characterizes the onset of macroscopic damage [9, 10]. The critical pressure responsible for the appearance of second peak is between 1.7-2 bar. For non-damaging tests, the fall of strain rate reaches negative values, which correspond to the springback in the sample. Figure 5 shows the stress/strain for nine strain rates of 224, 339, 439, 454, 545, 603, 656, 700 and 882 s^{-1} which correspond respectively to 0.5, 0.7, 1, 1.2, 1.5, 1.7, 2, 2.2 and 2.5 bar impact pressure. Dynamic compressive behavior of the composite is strongly influenced by the strain rate. The stress-strain behavior in each case was similar during the linear elastic behavior, whereas the stress increased with the increasing strain rate. For non-damaging tests, we observed that the sample tends to take again its initial state, with presence of plastic deformation. On the other side, for damaging tests, the sample continues to deform. Also, a brittle behavior is noted, which is controlled by matrix failure. The nonlinearity of the stress-strain curves is different and corresponds to different damaging modes. From Figure 5, the Young modulus, maximum compressive stress and failure strain have been obtained and listed in Table 2. For in-plane loading, the dynamic stiffness $E_{dynamic}$ remains almost constant and the maximum stress σ_{max} increases with the impact pressure until a pressure threshold is reached from which the tendency is reversed; i.e. they decrease with the increase of impact pressure. The thermal softening due to inelastic heat dissipation and damage may explain this

behavior. Similar behavior has been reported by Tarfaoui [15] for SHPB testing of Glasse/Epoxy laminated composites.

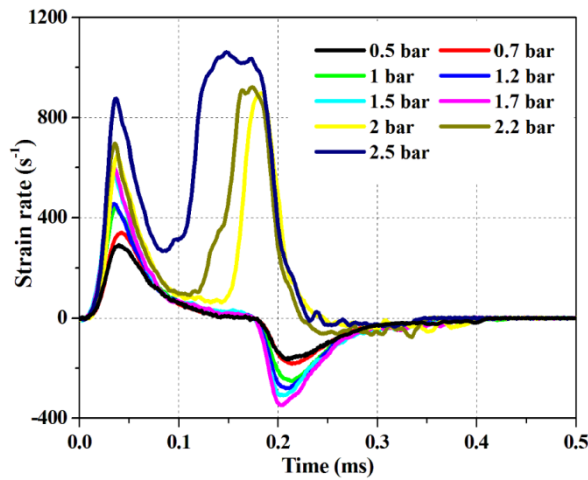


Figure 4. The strain rate–time curves of the specimen under in-plane loading

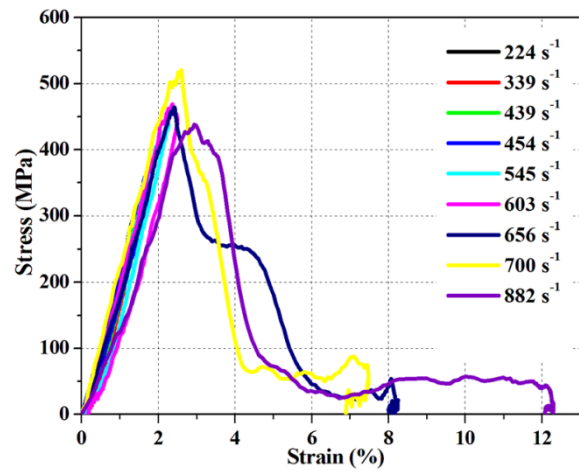


Figure 5. The stress–strain curves of the specimen under in-plane loading

| Strain rate (s^{-1}) | Young modulus (GPa) | Maximum stress (MPa) | Maximum strain (%) |
|--------------------------|---------------------|----------------------|--------------------|
| 293 | 21.01 | 207.58 | 1.1 |
| 339 | 21.67 | 297.30 | 1.7 |
| 439 | 21.27 | 355.92 | 1.9 |
| 454 | 21.91 | 390.38 | 2.1 |
| 545 | 21.31 | 436.62 | 2.4 |
| 614 | 21.10 | 475.91 | 2.6 |
| 903 | 19.94 | 481.34 | 2.8 |
| 922 | 21.58 | 519.71 | 2.8 |
| 1061 | 16.49 | 445.43 | 3.5 |

Table 2. Mechanical properties of the woven composites subjected to in-plane loading

3.2 Out-of-plane test

3.2.1 Mechanical behavior

The out-of-plane dynamic compression response of the materials was also investigated. Figure 6 gives the evolution of the strain rate of $[0^\circ/90^\circ]_{26}$ samples for seven impact pressures. This figure shows the same likely than to in-plane tests. For undamaging tests, the fall of strain rate passes by negative values, which correspond to the springback in the sample. On the other hand, the appearance of a second peak characterizes the onset of macroscopic damage. The critical impact pressure at which the second peak appears is between 5.17–5.25 bar (respectively 1813 – $1902 s^{-1}$). The compressive stress-strain curves at strain rate from 659 to $1902 s^{-1}$ for the composites are presented in Figure 7. From this figure, the Young modulus, maximum stress and failure strain have been obtained and listed in Table 3. It is observed also an increase of the mechanical properties, stress and strain, with the increase of the strain rate. However, the elastic modulus seems not to change before the appearance of the damage.

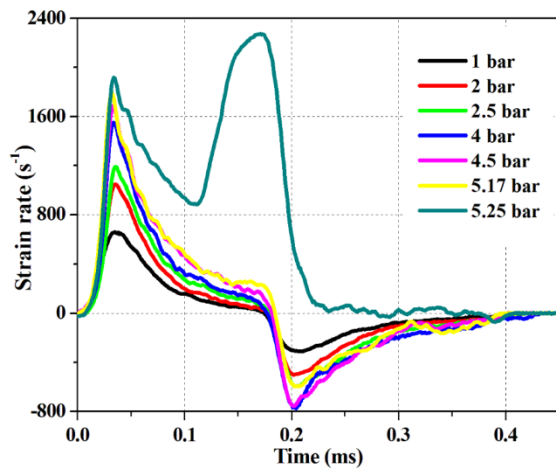


Figure 6. The strain rate–time curves of the specimen under out-of-plane loading

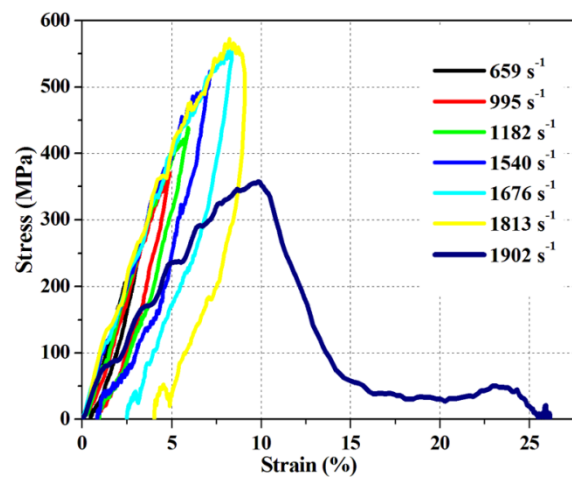


Figure 7. The stress–strain curves of the specimen under out-of-plane loading

| Strain rate (s^{-1}) | Young modulus (GPa) | Maximum stress (MPa) | Maximum strain (%) |
|--------------------------|---------------------|----------------------|--------------------|
| 659 | 8.64 | 263.80 | 2.56 |
| 995 | 8.74 | 381.56 | 5.54 |
| 1012 | 8.27 | 386.09 | 5.85 |
| 1182 | 8.11 | 435.22 | 6.67 |
| 1540 | 7.95 | 518.00 | 8.20 |
| 1676 | 7.55 | 551.99 | 9.80 |
| 1813 | 7.50 | 565.74 | 9.60 |
| 1902 | 4.05 | 357.43 | 11.00 |

Table 3. Mechanical properties of the woven composites subjected to out-of-plane loading

4 NUMERICAL SIMULATION

4.1 FE model

Split Hopkinson Pressure Bar tests were modeled to study the stress wave propagation and dynamic deformation of the composite materials. Commercially available finite element software ABAQUS was used throughout the numerical studies. Considering the arrangement showed in Figure 2 and taking into account the dimensions of the equipment available in the Ship Structures Mechanics Laboratory of the ENSTA Bretagne, both incident and transmitted bar were modeled with a diameter of 20 mm and a length of 1985 mm and 1948 mm, respectively. Likewise, the striker had 400 mm in length and the same diameter. The incident, transmitted and the striker bars were modeled as an isotropic elastic material. Meanwhile the specimen was a common size of $13 \times 13 \times 10 \text{ mm}^3$ and was modeled with an orthotropic elastic material. This composite specimen is made up of 52 stacked plies $[0^\circ/90^\circ]$ with a ply thickness of 0.195 mm. An assembly containing all parts (bars, striker and specimen) was modeled using three-dimensional solid 8-node linear brick elements, with reduced integration and hourglass control (C3D8R in ABAQUS library). The incident, transmitted and the striker bars had uniform mesh into 104192, 97870 and 21890 elements, respectively. The specimen is meshed into 8788 elements. Mesh configuration of the composite specimen appears in Figure 8, while in turn Figure 9 presents a detail of the full model assembly. At the interfaces of different parts of the SHPB setup, a surface to surface contact is defined to simulate the interaction at these interfaces, allowing for compressive loads to be transferred between the

slave nodes and the master segments. Material properties used in the finite element code are shown in Table 4 and Table 5. The skins with a negligible thickness acting as gauges were placed on incident and transmitted bars, with the purpose to determine the incident, transmitted and reflected waves. These skins were modeled using the mesh with membrane elements M3D4R (A 4-node quadrilateral membrane, reduced integration, hourglass control). Initial velocity conditions were applied to the whole striker volume (all nodes), whose value exactly corresponded to the actual one, e.g. $V=5$ m/s. Initial boundary conditions were applied to the striker and the bars such that only movement in one direction was allowed. The different physical parameters (loads, velocities, strains...) can be determined by the numerical model and compared with experimental results:

- The loads " F_i " and " F_t " are determined at the incident and transmitted bar in contact with the specimen, the loads are deduced from the values of stress applied at the nodes of each of the elements.
- The incident velocity " V_i " and transmitted velocity " V_t " of the bar are deduced at the surface of contact between the incident and transmitted bars with the specimen, Figure. 10.

| Material | Density (Kg/m ³) | Young's modulus (GPa) | Poisson's ratio | Elastic wave speed, (m/s) |
|------------------|------------------------------|-----------------------|-----------------|---------------------------|
| Steel (Maraging) | 7819 | 183.9 | 0.32 | 4849.70 |

Table 4: Material properties of bar materials used in numerical study

| E_1 (MPa) | E_2 (MPa) | E_3 (MPa) | ν_{11} | ν_{23} | ν_{13} | G_{12} (MPa) | G_{13} (MPa) | G_{23} (MPa) |
|-------------|-------------|-------------|------------|------------|------------|----------------|----------------|----------------|
| 23711 | 23711 | 9000 | 0.151 | 0.2 | 0.2 | 4498 | 1456 | 1456 |

Table 5: Material properties of the composite

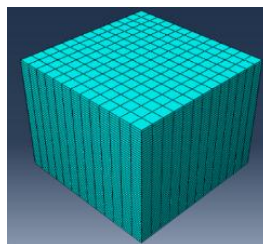


Figure 8. Mesh configuration of composite specimen

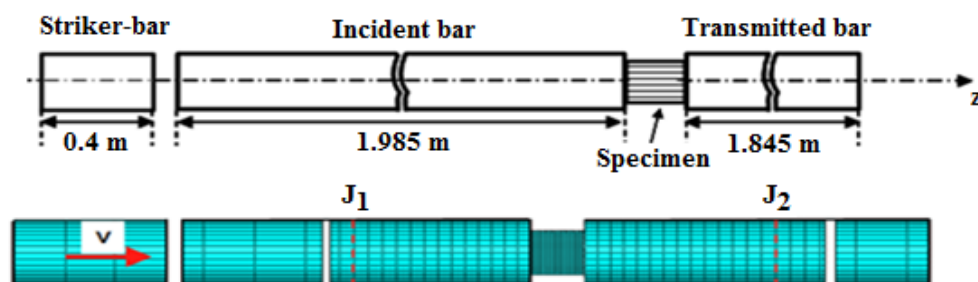


Figure 9. Numerical model of SHPB apparatus

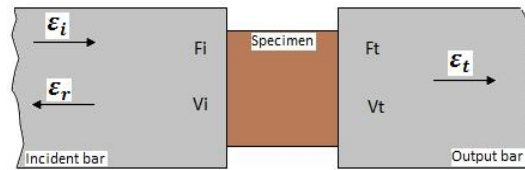


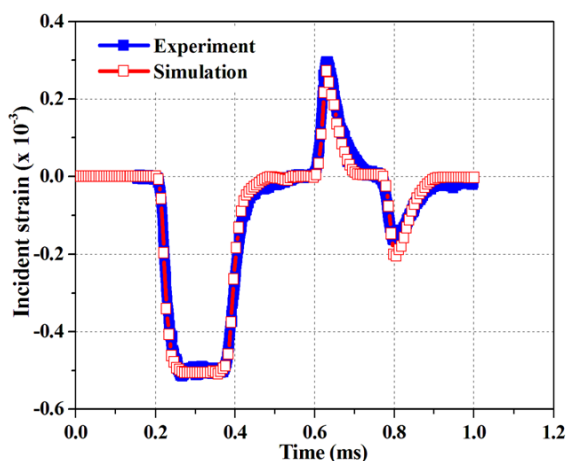
Figure 10. Correlation parameters of the model

4.2 Results of Numerical Study

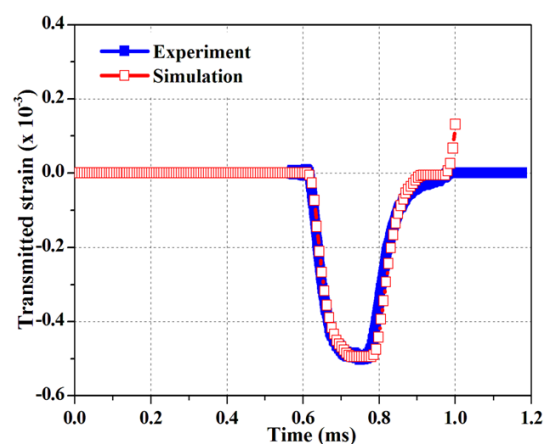
SHPB experiments conducted with composite were numerically modeled using ABAQUS finite element software. The SHPB experiments done with composite subjected to in-plane and out-of-plane were compared with the numerical study which is presented in Figure 11. In this figure, blue curve represents the SHPB experiment of the composite while red curve represents the result of numerical study and both curves were shifted in time domain to simplify distinguishing. In general, a good agreement between the measured results and finite element results is observed for in-plane loading direction.

For in-plane simulations, the strain of incident and reflected compression wave measured by the gauge J_1 , gives a good estimate of the experimental results. This also applies for incident and transmitted velocity. Indeed, the numerical velocity is taken at the incident surface of the bar in contact with the sample. The evolution of the incident and transmitted loads, given at two interfaces of the bars in contact with the sample are well simulated. We have the same rise and fall of the load, but we haven't the same level of the maximum load. At the experimental and numerical results we find a slight general difference which may be related to the experimental conditions:

- the geometry of the samples is not perfectly cubic,
- the parallelism of the faces in contact with the bars,



(a) Incident strain



(b) Transmitted strain

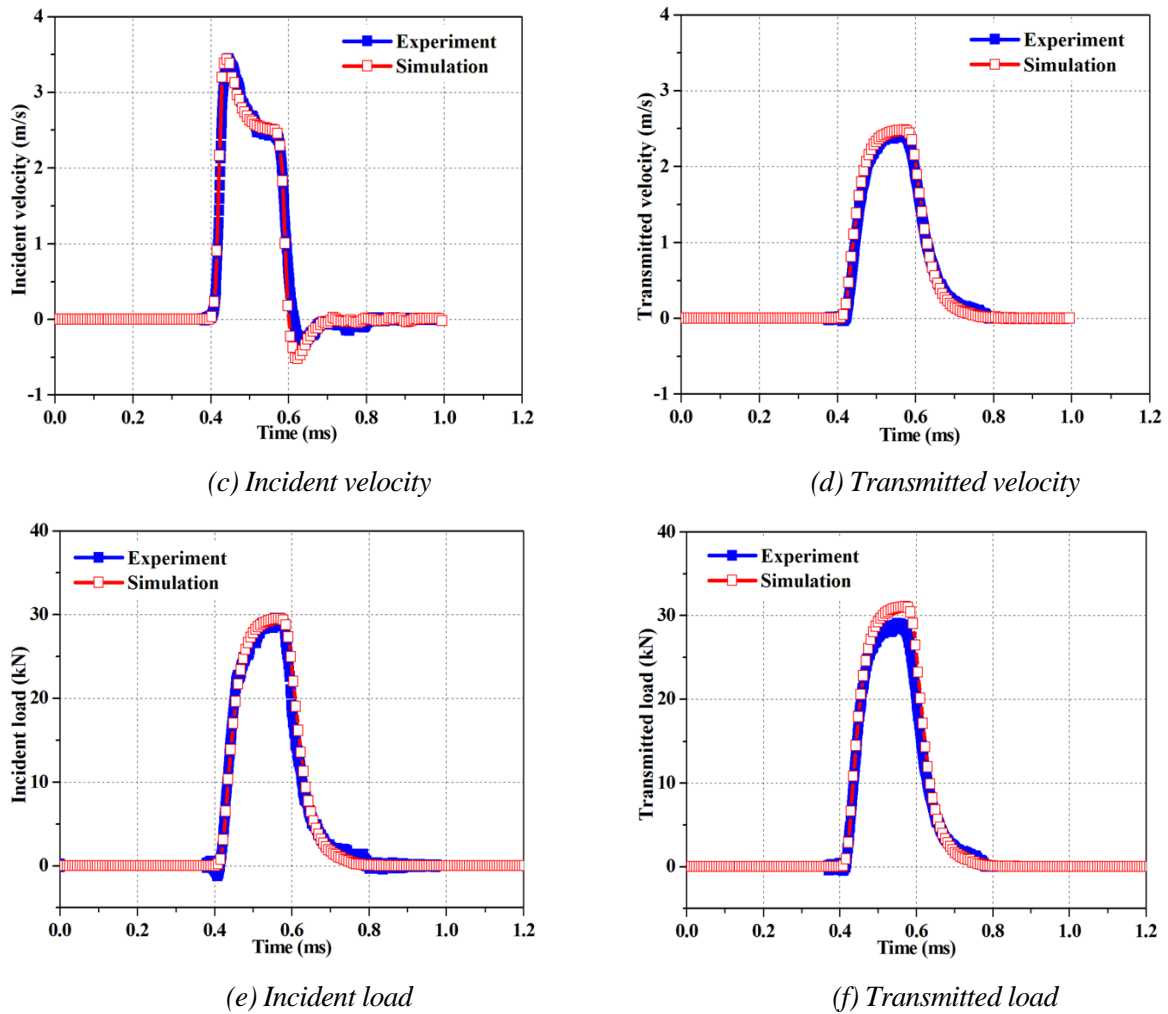


Figure 11. Experimental and numerical results, in-plane test, $P=0.5$ bar.

5 CONCLUSION

A Split Hopkinson pressure bar was used to conduct high compressive strain rate experiments. Samples were subjected to in-plane (IP) and out-of-plane (OP) tests. The first observation can be made, for IP and OP tests, is that materials show a strength dependency on loading direction and impact pressure. Moreover, the stress-strain curves manifest significant influence of the strain rate on the composite mechanical behavior. The maximal stresses achieved depend on the strain rate; the higher the strain rate, the higher the stress level. The maximal stresses obtained both during dynamic compression tests are higher for the composite subjected to out-of-plane loading. Damage appears only for specific impact pressure on the samples: 1.7 - 2 bar for in-plane loading and 5.17 - 5.25 bar for out-of-plane loading.

In the second part of this study, a three-dimensional numerical model of the SHPB test including the incident bar, transmitter bar, the projectile and the specimen was developed. The dynamic compression response was simulated using ABAQUS structural analysis software. Numerical models without damage were developed and successfully predicted the elastic behavior of the materials. The results predicted by the numerical simulation are consistent with observed experimental results with a slight difference, which may be related to the experimental conditions: the geometry of the samples is not perfectly cubic, the parallelism of

the facets in contact with the bars.... This study is to be completed by developing the model which takes into account the damage.

ACKNOWLEDGEMENTS

The Authors of this paper gratefully acknowledge the financial support of the DGA, France (MRIS project).

REFERENCES

- [1] L. Ninan, J. Tsai, C.T. Sun. Use of split Hopkinson pressure bar for testing off-axis composites, *International Journal of Impact Engineering*.25: 291-313, 2001
- [2] H. Kolsky, An investigation of the mechanical properties of materials at very high rates of loading, *Proc. phys. Society*. 62: 676-700, 1949.
- [3] L.J. Griffiths, D.J. Martin. A study of the dynamic behaviour of a carbon–fibre composite using the split Hopkinson pressure bar, *Journal of Physics*.7:2329–41, 1974.
- [4] X. Chen, X. Li, Z. Zhi, Y. Guo, N. Ouyang. The compressive and tensile behavior of a 0/90 C fiber woven composite at high strain rates, *Carbon*.61: 97–104, 2013.
- [5] M.V. Hosur, J. Alexandre, U.K. Vaidya., S. Jeelani.High Strain Rate Compression Response of Carbon/Epoxy Laminate Composites.*Journal of Composite Structures*, 52: 405-417, 2001.
- [6] C.E. Lanchezhian, B. Vijaya Ramnath, J. Hemalatha. Mechanical behaviour of glass and carbon fibre reinforced composites at varying strain rates and temperatures, *Procedia Materials Science*. 6 : 1405–1418, 2014.
- [7] R.L. Sierakowski, G.E. Nevill, C.A. Ross, E.R. Jones. Dynamic Compressive Strength and Failure of Steel Reinforced Epoxy Composites.*Journal of Composite Materials*, 5: 362-377, 1971.
- [8] S.T. Jenq, S.L. Sheu, High Strain Rate Compressional Behavior of Stitched and Unstitched Composite Laminates with Radial Constraint, *Composite structure*. 25: 427-438, 1993.
- [9] M. Tarfaoui, S. Choukri, A. Neme.Effect of fibre orientation on mechanical properties of the laminated polymer composites subjected to out-of-plane high strain rate compressive loadings, *Composite Science and Technology*. 68 : 477-485, 2008.
- [10] M. Tarfaoui, S. Choukri, A. Neme.Damage kinetics of glass/epoxy composite materials under dynamic compression, *Journal of Composite Materials*. 43: 1137-1154, 2009.
- [11] A.M.A. El-Habak. Mechanical behaviour of woven glass fibre-reinforced composites under impact compression load.*Composites*, 22 : 129–134, 2001.
- [12] E. Woldenbet, J.R. Vinson. Effect of specimen geometry in high strain rate testing of graphite/epoxy composites, *In: Proceedings of the 38th AIAA/ASME/ASCE/AHS/ASC Struc Struc Dyn and Matl Conf*. 2 : 927-934, 1997.
- [13] J. Harding. Effect of strain rate and specimen geometry on the compressive strength of woven glass-reinforced epoxy laminates.*Composites*, 24 : 323–432 , 1993.
- [14] Abaqus 6.12: Analysis User's Manual.
- [15] M. Tarfaoui, Experimental investigation of dynamic compression and damage kinetics of Glass/Epoxy laminated composites under high strain rate compression, *Advances in Composites materials-Ecodesign and Analysis*, 16 : 359-382, 2011.